

Chromosome biorientation and APC activity remain uncoupled in oocytes with reduced volume

Simon I.R. Lane* & Keith T. Jones

Biological Sciences, Faculty of Natural and Environmental Sciences, University of Southampton, Southampton SO17 1BJ, UK and School of Biomedical Sciences & Pharmacy, University of Newcastle, 2290, Australia.

*Correspondence: simon.lane@soton.ac.uk

+44 (0)2380 594257

Biological Sciences, Faculty of Natural and Environmental Sciences, University of Southampton, Southampton SO17 1BJ, UK

Condensed title: Influence of mammalian oocyte size on the SAC

Abstract

The spindle assembly checkpoint (SAC) prevents chromosome mis-segregation by coupling anaphase-onset with correct chromosome attachment and tension to microtubules. It does this by generating a diffusible signal from free kinetochores into the cytoplasm, inhibiting the anaphase-promoting complex (APC). The volume in which this signal remains effective is unknown. This raises the possibility that cell volume may be the reason why the SAC is weak, and chromosome segregation error-prone, in mammalian oocytes. Here, by a process of serial bisection, we analyzed the influence of oocyte volume on the ability of the SAC to inhibit bivalent segregation in meiosis I. We were able to generate oocytes with cytoplasmic volumes reduced by 86% and observed changes in APC activity consistent with increased SAC control. However, bivalent biorientation remained uncoupled from APC activity, leading to error-prone chromosome segregation. We conclude that volume is one factor contributing to SAC weakness in oocytes. However additional factors likely uncouple chromosome biorientation with APC activity.

Introduction

To be effective against chromosome mis-segregation, the spindle assembly checkpoint (SAC) must prevent anaphase until all chromosomes are correctly attached to spindle microtubules, a state called biorientation (Foley and Kapoor, 2013; Musacchio, 2015). It does this by using free kinetochores as a platform for generating a diffusible inhibitor of the anaphase-promoting complex (APC), a cytoplasmic mitotic checkpoint complex (Jia et al., 2013; Pesenti et al., 2016). One would imagine in a robust checkpoint such as that exhibited by somatic cells, the inhibitory signal would prevent APC activity throughout the entire cytoplasm. However, there may be a limit on how far the signal can diffuse before it becomes too dilute to be effective. Previous work in PtK1 cells has shown an inability of a non-biorientated chromosome on one spindle to influence anaphase onset on an adjacent spindle in a shared cytoplasm (Rieder et al., 1997), raising the possibility of a limit on the effective distance of the inhibitory signal. More recent studies in fused cells show that the strength of the SAC is also diminished by both diffusion barriers and dilution by non-mitotic cytoplasm (Heasley et al., 2017).

Oocytes are much larger than somatic cells, raising the question of how the SAC can regulate the APC within this much larger volume. It is possible that in such large cells the SAC cannot fully inhibit APC activity. Indeed, in *Xenopus* eggs, which are ~1mm in diameter, there does not appear to be any influence of the SAC on the meiotic divisions (Liu et al., 2014; Shao et al., 2013). However, SAC activity can be restored by raising the nuclear:cytoplasmic ratio by adding sperm nuclei to cytoplasmic *Xenopus* egg homogenates (Minshull et al., 1994). Furthermore in the developing embryos of a number of species including *Xenopus*, *C. elegans* and zebrafish there is considerable interest in cell size and developmental timers on the establishment of the SAC during embryogenesis (Galli and Morgan, 2016; Zhang et al., 2015; Clute and Masui, 1995).

Mammalian oocytes are typically 70-150 μm in diameter dependent on species and are large enough to present a volume in which the predicted

reach of the SAC is exceeded. In contrast to *Xenopus*, the SAC is certainly physiologically active during the meiotic divisions of mammalian oocytes, and as such knockdown/knockout of any one component of the checkpoint raises aneuploidy rates (Hached et al., 2011; Homer et al., 2005; McGuinness et al., 2009). However, it is generally regarded that the SAC is weak in its surveillance of mis-alignment or non-attachment, because it cannot prevent anaphase when a small number of bivalents are not biorientated in mouse oocytes (Lane et al., 2012; Gui and Homer, 2012; Kolano et al., 2012; Sebestova et al., 2012; Nagaoka et al., 2011). Such loss of APC control by a weak SAC would account for the higher rates of aneuploidy observed in oocytes during their first meiotic division (meiosis I; (Jones and Lane, 2013; Gorbsky, 2015; Touati and Wassmann, 2016; Merriman et al., 2013). Indeed the control of the APC by the SAC appears weak enough that during the major part of meiosis I when the APC is at its greatest measureable activity, the SAC is still partially on (Lane and Jones, 2014). All these observations collectively point to mammalian oocyte size being an important factor that limits the ability of the SAC to inhibit the APC.

Recently, it has been shown that a reduction in the size of mouse oocytes by a half enforces the SAC, if the volume reduction occurs before nuclear envelope breakdown (NEB) (Kyogoku and Kitajima, 2017). However the reduction in oocyte volume occurs also with a concentration of SAC components, being formed at the nuclear envelope. Here we set out to test the strength of the SAC generated by the (pro)metaphase kinetochores, without the confounding effects of enriching SAC components, by using a procedure of repeatedly bisecting oocytes after NEB to achieve a highly miniaturised cell with a volume reduced by ~86%. We find the spindle scales in proportion to the cytoplasmic volume, and the timing of APC activation is delayed, however it still remains uncoupled from the normal process of bivalent biorientation. Subsequent use of low doses of spindle poison in a reduced volume decrease bivalent biorientation success and activates the SAC to a greater extent than in large oocytes. We demonstrate that the volume limit at which the SAC signal from individual bivalents might be effective is far less than $\sim 1/8^{\text{th}}$ that of a normal mouse oocyte (<27pL).

Results and Discussion

To examine the influence that cell volume has on the ability of the SAC to arrest mouse oocytes in meiosis I, we first set about producing oocytes of varying size. We established a serial bisection technique using cytochalasin D, which has been used previously for halving oocytes in a single procedure (Hoffmann et al., 2011; Polanski and Kubiak, 2013). Immediately following NEB, oocytes could be bisected up to 3 times, and we defined these products as B₁, B₂, and B₃ oocytes (Bisected once, Bisected twice, or Bisected three times), which created cells of $\frac{1}{2}$, $\frac{1}{4}$ and $\frac{1}{8}$ their original volume respectively (**Fig. 1 A**). We also produced serially sham-bisected oocytes (B₀), where the bisection procedure was aborted just prior to cleaving the oocyte in two. The two halves were still connected by a thin cytoplasmic bridge and reformed a single spherical shape within 1-2 minutes (data not shown). The bisection procedure was reproducibly accurate, with serially bisected oocytes having volumes of 190±17pL (B₀), 93±15pL (B₁), 50±11pL (B₂) and 27±6pL (B₃), and radii of 36±1µm (B₀), 28±1µm (B₁), 23±2µm (B₂) and 18±1µm (B₃; **Fig. 1, B and C**). Chromosome counts demonstrated that 95% (n=20) of B₃ oocytes contained the correct number of 20 bivalents following triple bisection; showing that the chromosomes had not been dispersed during the procedure (**Fig. S1, A and B**).

In order to verify that their reduced volume did not affect the ability of the oocyte to form a spindle, we microinjected cRNA for histone2B (H2B)-mCherry and β-tubulin-GFP. Oocytes were examined at 7h after NEB, a time when spindles are fully formed (Schuh and Ellenberg, 2007). We observed normal anastral barrel-shaped spindle morphology independent of volume (**Fig. 1 D**). Overall, both spindle pole-to-pole length and equatorial width declined as oocytes became smaller (**Fig. S1 C**), such that the ratio of spindle volume to oocyte volume remained relatively constant (**Fig. S1 D**). Therefore, spindles of mammalian oocytes demonstrate the same ability to scale in proportion to cell size as do *Xenopus* eggs (Good et al., 2013; Hazel et al., 2013). Importantly, the serial bisection procedure had no impact on the ability of oocytes to complete meiosis I, with 60-70% extruding a polar body (PBE) independent of size (**Fig. 1 E**).

In summary, we have established a procedure that can reduce the volume of an oocyte eight-fold. The resulting volume is still larger than a somatic cell (27 pL here versus ~0.1-10 pL for various mammalian cells). However the reduced volume of the B₃ cell raises the possibility that the SAC signal may be able to penetrate the cytoplasm at sufficient concentration to increase the efficacy of the SAC.

To investigate whether reducing oocyte volume had changed the properties of the SAC, we measured the degradation of the APC substrate securin (Holt et al., 2013; Herbert et al., 2003). Following securin degradation in real-time gives a measure of APC activity, a process in oocytes that is not dependent on the presence of bivalents following serial bisection (**Fig. 2 A**). Such a finding is in agreement with previous studies on oocytes following a single bisection procedure (Hoffmann et al., 2011; Lane and Jones, 2014), and demonstrates that active APC is dispersed throughout the oocyte cytoplasm.

B₀ and B₃ oocytes expressing securin-YFP and H2B-mCherry, and containing bivalents, were imaged by timelapse microscopy to record securin loss and monitor bivalent segregation at anaphase (**Fig. 2 B**). For each oocyte, the time of NEB and anaphase were recorded, as well as the point at which securin degradation was initiated between these two events. The initiation of securin loss we term 'APC activation'. B₃ oocytes spent significantly more time in meiosis I (measured as the interval between NEB and anaphase) when compared to B₀ (B₃, 9.8±1.8h; B₀, 9.0±1.3h; P=0.0234 **Fig. 2 C**). However, more striking differences were observed when the period between NEB and APC activation was measured, as well as the period between APC activation and anaphase (**Fig. 2 D**). Comparison of these timings in B₀ and B₃ oocytes revealed securin remained stable significantly longer in the B₃ oocytes (B₀, 6.6±0.9h; B₃, 7.9±1.7h; P<0.0001), but was then subsequently degraded in a significantly shorter time (B₀, 2.4±0.7h; B₃, 1.8±0.4h; P=0.0002). Consistent with this we found that in percentage terms the peak APC activity was significantly greater in the B₃ oocytes (B₀, 48.9±9.15%h⁻¹; B₃, 62.1±22.5%h⁻¹; P=0.0007; **Fig. 2, E-F**).

The above observations suggest that APC regulation was subtly changed in a reduced oocyte volume, such that there was a longer period of prometaphase, in which the APC is not active but then a shorter metaphase-anaphase transition, due to raised APC activity. This is somewhat reminiscent of the more switch-like transition in APC activity seen in mitotic cells (Clute and Pines, 1999); and it would be a finding that would be consistent with the SAC having greater control over the APC during prometaphase, before the APC is active. However, many other interpretations are possible in explaining why the periods of NEB-APC activation and APC activation-anaphase differ. For example, there may have been changes in the ability to assemble a smaller, more crowded, spindle in B₃ oocytes or differences in the segregation of any protein between nucleoplast and cytoplasm, which may have impacted on the timing of meiosis.

We decided to test if the change in the timing of APC activation during meiosis I in B₃ oocytes was because the SAC was more effective in inhibiting the APC in the presence of non-biorientated bivalents. If so, one would expect to observe only biorientated bivalents during the 2-3 h of APC activity preceding anaphase (**Fig. 2 E**). However, 4D-CLSM imaging of live oocytes expressing H2B-mCherry and CenpC-GFP at this time, revealed several examples of bivalents moving on and off the spindle equator, showing them to be in the process of establishing biorientation (**Fig. 3 A**, see arrowheads; **and Video 1**). Three objective measurements of biorientation in live oocytes were made (**Fig. 3 B**): bivalent stretch (distance between the kinetochore pairs), displacement (from the metaphase plate) and θ (angle bivalent intersects the metaphase plate). For each bivalent these measures were compared against those of fully biorientated control oocytes matured to metaphase (8 hours post NEB, Collins et al., 2015). Bivalents greater than 3 standard deviations away from the mean control values in any of the three measures were considered as non-biorientated. Using this analysis we observed non-biorientated bivalents in live oocytes during the 2-3 hours prior to anaphase (**Fig. 3 C**) and even in the minutes immediately before anaphase (**Fig. 3, C and D; and Video 1**). In addition we found no significant differences between B₀ and B₃

oocytes at any of the timepoints assessed in terms of the number of non-biorientated bivalents per oocyte (**Fig. 3, C, E and F**), suggesting the reduced volume was not significantly affecting the ability of bivalents to biorientate.

The presence of non-biorientated bivalents during the period of APC activity in B_3 oocytes suggests that reducing oocyte volume had not had any beneficial effect on the ability of the SAC to inhibit the APC in response to a small number of attachment errors. We were not technically able to bisect B_3 oocytes further to determine if reducing the oocyte volume below 27pL had any greater impact on the dynamics of APC activity. However, we could increase the number of bivalents not biorientated using a low dose of the spindle poison nocodazole, which does not block anaphase in fully sized oocytes (Collins et al., 2015). We wondered if an increased number of non-biorientated chromosomes in conjunction with a reduced oocyte volume would provide a situation in which the SAC can restrain the APC.

B_3 and B_0 oocytes were cultured in 0 or 25nM nocodazole throughout meiosis I, and scored for PBE. Nocodazole at this dose caused a significant drop in PBE for B_3 but not for B_0 oocytes (B_3 , 34/50 vs 15/39, $P=0.0095$; B_0 , 69/104 vs 65/90, $P=0.7647$; **Fig. 4 A**). We reasoned B_3 oocytes could be more sensitive to nocodazole either because of an increased SAC efficiency, or because the nocodazole had a greater ability to disrupt bivalent biorientation in B_3 than in B_0 oocytes. Upon examination of the bivalents we favoured the latter explanation as non-biorientated bivalents were always observed at a greater frequency in the B_3 oocytes: in the 2 hours preceding anaphase, B_0 oocytes had between 0 and 4 (mean=1.6), while B_3 oocytes had between 3 to 12 (mean=5.4; **Fig. 4, B and C; and Video 2**). The ability of nocodazole to have a greater disruptive influence on the spindle of B_3 oocytes, may be because the drug penetration is greater in a smaller volume (there is a 2x greater surface area: volume ratio in a B_3 oocyte versus a B_0 oocyte), or due to a greater ability to impact on a smaller and more crowded spindle (**Fig. 1 D**). As such in B_3 oocytes, 29% of the bivalents were classified as non-biorientated. Furthermore, 5 minutes before anaphase, 25% of bivalents

remained non-biorientated (**Fig 4D,E**) demonstrating that these chromosomes persistently failed to attach correctly to the spindle.

We next sought to adjust the nocodazole concentration such that both B₀ and B₃ oocytes experienced very similar levels of bivalent disruption, thus allowing a comparison of their SAC efficacy. B₃ oocytes treated with 25nM nocodazole were compared to B₀ oocytes treated with varying doses of nocodazole at 7 hours after NEB (**Figs. 5, A-C and S2**). We found that 35nM Nocodazole in B₀ oocytes gave the closest match to 25nM in B₃ oocytes (**Fig. 5, B and C**). Under these conditions of matched bivalent disruption we found that B₃ oocytes were more likely to arrest in MI (B₀, 6/36; B₃, 18/43; P=0.026; **Fig. 5 D**). In those oocytes that did extrude polar bodies, there was no significant difference in the duration of meiosis I (B₀, 10.5±1.8, n=30; B₃, 11.0±1.6, n=25; P=0.3237; **Fig. 5 E**).

On examination of the securin destruction profiles in both B₀ and B₃ oocytes treated with nocodazole it was apparent that there were two patterns of degradation (**Fig. 5, F and G**). Firstly a typical profile, very similar to oocytes not treated with nocodazole, whereby securin is degraded continuously after APC activation resulting in anaphase within a few hours (**Fig. 5 G**, blue trace). However, a second profile with transient switches from degradation to net synthesis of securin was commonly observed. We termed this event 'stalling' and defined it as a period of at least 20 minutes during which degradation dropped to less than 15% per hour of securin (**Fig. 5 G**, green/red trace). This stalling event was equally common amongst B₀ and B₃ oocytes that arrested in MI, but was significantly more common in B₃ oocytes than in B₀ in those oocytes that completed meiosis I (MI arrest B₀, 3/6; MI arrest B₃, 10/18; P=1; PBE B₀, 3/30; PBE B₃, 15/25; P=0.0013; **Fig. 5, H and I**) and was associated only with oocytes treated with nocodazole, as it was never observed in untreated oocytes of any size (0/77 oocytes, data not shown).

We next used the securin traces to define the timing of APC activation and thus the length of prometaphase and metaphase, as we did for Fig. 2.

We found significant changes in these measures both between B₃ and B₀ oocytes with or without nocodazole, and also between those oocytes experiencing stalling and those not (**Fig. 5 J and S3**). Nocodazole addition resulted in modest increases in the duration of prometaphase and metaphase for both B₀ and B₃ oocytes when the non-stalled metaphase oocytes were considered. However for both sizes of oocyte stalling was associated with a much longer duration of MI, with increases predominantly in the time spent in metaphase (B₀ stalled, 6.5±1.2, n=3; B₀ non-stalled, 3.1±1.3, n=27; P<0.0001; B₃ stalled, 4.7±1.4, n=10; B₃ non-stalled, 2.3±0.7, n=15; P<0.0001). It is of note that in our experiment only 3 B₀ oocytes experienced stalling therefore changes to the timing of meiosis I in this group should be viewed with caution. A detailed analysis of statistical comparisons between all groups can be found in **Fig. S3**.

In summary we find that when oocytes are exposed to doses of nocodazole designed to elicit a controlled disturbance to bivalent biorientation, the reduced size of the B₃ oocyte can temporarily stop the activity of the APC. This stalling of the APC was never seen in the absence of nocodazole and was rarely seen in full size oocytes, suggesting that both the reduction in size and the additional stimulus of disrupted bivalents are required for an oocyte to inhibit the APC.

In summary, we have used a serial bisection technique to reduce the volume of mouse oocytes by more than 85%. It did not affect their ability to complete meiosis I. However, it did result in a change in the size of the spindle, which reduced in proportion with oocyte volume, consistent with previous reports (Good et al., 2013; Hazel et al., 2013; Kyogoku and Kitajima, 2017). In small oocytes we observed differences in APC timing (~1.4 h later securin degradation onset) and activity (~20% greater). One explanation of these findings is that an increased concentration of the kinetochore-derived SAC signal in a reduced volume causes greater control of the APC. This is consistent with the finding that the SAC strength grows as cells become smaller in the *C. elegans* embryo (Galli and Morgan, 2016) and that checkpoint function must depend on a balance between the relative SAC and APC strength (Wild et al., 2016). However, in small oocytes, as in full-sized

oocytes, low doses of spindle poison generate large numbers of non-biorientated bivalents that do not prevent anaphase (Kolano et al., 2012; Gui and Homer, 2012; Sebestova et al., 2012; Lane et al., 2012; Nagaoka et al., 2011). Complete arrest in meiosis I may not be expected however as even in mitotic cells the SAC is not absolute in its ability to prevent anaphase, and demonstrates a graded response proportional to the stimulus (Collin et al., 2013; Dick and Gerlich, 2013; Heinrich et al., 2013). A ~10-fold increase in the mean number of non-biorientated bivalents per small oocyte (5.4 versus 0.5) caused only transient blocks to APC activity and thus did not prevent anaphase. We conclude that volume is not the only factor that uncouples chromosome biorientation from APC activity in oocytes.

Kyogoku and Kitajima have demonstrated that a robust checkpoint can be enforced only if oocyte volume is reduced prior to NEB (Kyogoku and Kitajima, 2017). This enriches the mitotic checkpoint complex (MCC) in the half-oocyte containing the nucleus, because it is generated at nuclear pores (Rodriguez-Bravo et al., 2014; Kyogoku and Kitajima, 2017). In addition, other checkpoint kinases are known to have roles in G2 that influence the SAC efficacy in mitosis (Yu et al., 2017), and so may also be enriched by halving before NEB. In our study the reduction in volume was performed after NEB, and thus is more likely to reflect the ability of kinetochores to prevent anaphase with unperturbed concentrations of cytoplasmic APC inhibitors. In agreement with Kyogoku and Kitajima, we find evidence that reduced volume can increase the ability of the SAC to control APC activity, implying size is a factor in explaining the weak spindle checkpoint of mammalian oocytes. However by our method the APC could not be inhibited sufficiently so as to prevent anaphase in response to non-biorientated bivalents, even when many persisted over long periods of time. Therefore factors, such as low levels of pre-formed MCC at NEB, could play a role in the weakness of the SAC in oocytes.

Materials and Methods

All reagents were from Sigma-Aldrich, UK unless otherwise stated.

Animals and oocyte culture. Four- to six-week-old C57BL/6 mice were used throughout. Oocytes were collected from mice 48-52 h after injection with 10 IU pregnant mares serum gonadotropin (Centaur Services, UK) in M2 media (Fulton and Whittingham, 1978) under mineral oil. Milrinone (1 μ M) was added to maintain GV stage arrest (Tsafriri et al., 1996). NEB in oocytes was synchronized by incubation in milrinone for 2 h during which microinjections were performed if necessary. Followed washout of milrinone the timing of NEB was recorded by eye at 10 minute intervals. Oocytes not undergoing NEB within the modal time \pm 10 minutes were discarded from further study. Imaging and maturation studies were performed in M2 media at 37°C.

cRNA manufacture. cRNA was transcribed in vitro from purified, linear dsDNA template using a mMessage T3 (H2B-mCherry, Securin-YFP, Tubulin-GFP) or T7 (CenpC-GFP) RNA polymerase kit (Ambion, UK) (Lane and Jones, 2014). cRNA was suspended in nuclease-free water and its concentration determined by photospectrometry.

Microinjection. cRNA microinjections were conducted in M2 media covered in mineral oil on the stage of an inverted TE300 microscope (Nikon, Japan), using a 37 °C heated chamber and micromanipulators (Narishige, Japan). cRNA was injected using timed pressure injections from a Picopump (World Precision Instruments) to achieve a size of 1-2% of the oocyte volume, with the following pipette tip cRNA concentrations (ng/ μ L): Securin, 500; H2B, 250; CenpC, 600; Tubulin, 500; (Holt et al., 2013; Levasseur, 2013).

Drug addition. Nocodazole, at the final concentrations indicated (0-60nM) was added to media after completion of bisections and persisted throughout the remainder of the experiment. A stock concentration of 400mM in DMSO was used giving a final concentration of \leq 0.015% DMSO. Partitioning of nocodazole into the mineral oil was minimized using glass bottomed 96-well imaging plates (MatTek, USA) with 200 μ L of M2 media capped with a minimal volume of mineral oil.

Confocal imaging and chromosome tracking. Following bisections, oocytes injected with Histone 2B- mCherry and either EGFP-CenpC or Securin-YFP cRNA were placed on the stage of a Leica SP8 confocal microscope equipped with environmental chamber at 37 °C in M2 media covered by mineral oil. Up to 20 three-dimensional images (17 320x320 pixel z-sections with 2.2- μ m spacing; 32.3 x 32.3 x 35.2 μ m) were acquired every 300 s using 40x objective (NA=1.3, oil emersion) and 9x zoom. Chromosome tracking by in-lab software (Python, python.org) that controlled the microscope via communication with the SP8's Matrix Screener module ensured the chromosomes remained in the center of the imaging volume throughout maturation (Lane et al., 2016). Securin-YFP and DIC images were also acquired every 300 s but with 0.75x zoom.

Image processing. Images from chromosome tracking experiments were processed using ImageJ macros by subtraction of a 2 pixel Gaussian blur from a 10 pixel Gaussian blur background as described elsewhere (Kitajima et al., 2011).

Oocyte bisection. Following washout of milrinone, but prior to NEB oocytes were prepared by removal of the zona pellucida using a brief incubation (~5 seconds with pipetting) in acid Tyrode's solution followed by three washes to remove traces of acid. Oocytes were then incubated in cytochalasin D (2mM) until NEB occurred. Bisections were performed immediately following NEB on 1% agar gels made with phosphate-buffered saline and then equilibrated with M2 media containing cytochalasin D (~2 μ M). Oocytes were either bisected up to three times, resulting in $\frac{1}{2}$, $\frac{1}{4}$ or $\frac{1}{8}$ parts or sham bisected three times by leaving a narrow cytoplasmic bridge which allowed the two halves to regroup (Figure 1A). Bisection was performed manually under a stereomicroscope with a heated stage (37 °C) using a fine fibre drawn from a glass pipette in a flame.

Chromosome counting B₃ oocytes injected with H2B-mCherry and CenpC-GFP were imaged by confocal microscope with 1 μ m z-sections during prometaphase (before chromosome congression on the spindle). Chromosomes were counted by labeling each kinetochore pair in the 3D stack

using lab-made ImageJ macros.

Chromosome biorientation analysis. Analysis of bivalent biorientation was done by registering kinetochore positions in 3D confocal stacks using in-lab ImageJ macros. Macros label kinetochores non-permanently in the images to prevent users registering the same kinetochore twice and allow the kinetochores belonging to the same bivalent to be registered in pairs. Using the kinetochore position data a subsequent macro implements a best-fit algorithm to determine the position and normal angle of the spindle equator. The position and direction of the spindle equator is then used to calculate the displacement from, and angle of intersection with, each bivalent giving measures of displacement and θ respectively. Inter-kinetochore distance or 'stretch' is calculated by as the 3D distance between the two kinetochores of each bivalent. Control oocytes matured to metaphase (NEB+8 h) were used to create a data set. The mean and standard deviations (s.d.) for bivalent stretch, displacement and angle of bivalents in this group were used to define a standard metaphase. Each bivalent in the experimental groups was compared to this standard. The number of s.d. away from the control mean was calculated for stretch, displacement and angle, and the worst performing metric used to color that bivalent. Colors were assigned as follows: If the worst metric is <1 s.d. from the mean is colored green; ≥ 1 s.d. and <2 s.d. colored yellow; ≥ 2 s.d. and <3 s.d. colored orange; and ≥ 3 s.d. colored red. So a bivalent with stretch and displacement within one s.d. of their respective control means, but with angle greater than 1 s.d. and less than 2 s.d. from the control mean would be colored yellow (<2 s.d. from the mean). These are the colors used in the scatter plots in Figs 3, 4, 5 and S2.

Volume calculations. Oocyte volume was calculated by measuring the diameter of the oocyte twice in a 2D image (height and width), then calculating the radius from the average. Radius (μm) was converted to volume (pL) volume using the formula $V = 4/3000 \cdot \pi \cdot r^3$. Spindle volume was calculated as $V = 4/3000 \cdot \pi \cdot \frac{1}{2}L \cdot \frac{1}{2}W^2$ where L was the long axis and W the short axis of the spindle.

Data analysis. Fluorescence intensities were recorded from regions of

interest encompassing the oocytes using ImageJ software and subsequently stored in Microsoft Excel spreadsheets. Fluorescence traces were background subtracted and then normalized with maxima at 100%.

APC activity. Empirical Securin-YFP degradation data were imported into Matlab (R2013a, MathWorks, USA). The timing of securin degradation onset ('APC activation') was determined such that timepoint 't' was the first timepoint at which there was a significant difference between the previous and the subsequent 15 readings. Curve fitting (Fourier 3) was used to fit the data in the region of securin degradation and the first differential of this was used to calculate the maximal rate of Securin-YFP degradation achieved.

Statistical analysis. Statistical analysis was performed using Prism software (GraphPad Software, USA). Analysis of variance was used with Tukey's multiple comparison test for normally distributed data or Dunn's multiple comparison test for non-parametric data.

Online supplemental material.

Fig. S1 shows the bisection procedure did not cause loss of bivalents, nor did it prevent formation of spindles with normal proportions. Fig. S2 shows the bivalent biorientation results for B_0 oocytes treated with various doses of nocodazole, in order to establish a dose matching B_3 biorientation in 25nM nocodazole. Fig. S3 shows the duration of meiosis I and the lengths of prometaphase and metaphase for B_0 and B_3 oocytes treated with or without nocodazole. Relates to Fig. 5 J and provides summary of statistically significant differences. Videos 1 and 2 show time-lapse of B_3 oocytes with labeled chromosomes and kinetochores during meiosis I with and without 25nM nocodazole respectively.

Acknowledgements

We thank Dr. Marie H el ene Verlhac for the gift of Tubulin-GFP.

This work was funded by a project grant to KTJ from the Australian Research Council (DP120100946). The authors declare no competing financial interests.

Author Contributions

SL conceived the study, designed and performed the experiments, and analysed the data. SL and KJ wrote the manuscript.

References

- Clute, P., and Y. Masui. 1995. Regulation of the Appearance of Division Asynchrony and Microtubule-Dependent Chromosome Cycles in *Xenopus laevis* Embryos. *Dev. Biol.* 171:273–285. doi:10.1006/dbio.1995.1280.
- Clute, P., and J. Pines. 1999. Temporal and spatial control of cyclin B1 destruction in metaphase. *Nat. Cell Biol.* 1:82–87. doi:10.1038/10049.
- Collin, P., O. Nashchekina, R. Walker, and J. Pines. 2013. The spindle assembly checkpoint works like a rheostat rather than a toggle switch. *Nat. Cell Biol.* 15:1378–85. doi:10.1038/ncb2855.
- Collins, J.K., S.I.R. Lane, J.A. Merriman, and K.T. Jones. 2015. DNA damage induces a meiotic arrest in mouse oocytes mediated by the spindle assembly checkpoint. *Nat. Commun.* 6:8553. doi:10.1038/ncomms9553.
- Dick, A.E., and D.W. Gerlich. 2013. Kinetic framework of spindle assembly checkpoint signalling. *Nat. Cell Biol.* 15:1370–7. doi:10.1038/ncb2842.
- Foley, E. a, and T.M. Kapoor. 2013. Microtubule attachment and spindle assembly checkpoint signalling at the kinetochore. *Nat. Rev. Mol. Cell Biol.* 14:25–37. doi:10.1038/nrm3494.
- Fulton, B.P., and D.G. Whittingham. 1978. Activation of mammalian oocytes by intracellular injection of calcium. *Nature.* 273:149–51.
- Galli, M., and D.O. Morgan. 2016. Cell Size Determines the Strength of the Spindle Assembly Checkpoint during Embryonic Development. *Dev. Cell.* 36:344–352. doi:10.1016/j.devcel.2016.01.003.
- Good, M.C., M.D. Vahey, A. Skandarajah, D.A. Fletcher, and R. Heald. 2013. Cytoplasmic volume modulates spindle size during embryogenesis. *Science.* 342:856–60. doi:10.1126/science.1243147.
- Gorbsky, G.J. 2015. The spindle checkpoint and chromosome segregation in meiosis. *FEBS J.* 282:2471–2487. doi:10.1111/febs.13166.
- Gui, L., and H. Homer. 2012. Spindle assembly checkpoint signalling is uncoupled from chromosomal position in mouse oocytes. *Development.* 139:1941–1946. doi:10.1242/dev.078352.
- Hached, K., S.Z. Xie, E. Buffin, D. Cladière, C. Rachez, M. Sacras, P.K. Sorger, and K. Wassmann. 2011. Mps1 at kinetochores is essential for

- female mouse meiosis I. *Development*. 138:2261–2271.
doi:10.1242/jcs.092858.
- Hazel, J., K. Krutkramelis, P. Mooney, M. Tomschik, K. Gerow, J. Oakey, and J.C. Gatlin. 2013. Changes in cytoplasmic volume are sufficient to drive spindle scaling. *Science*. 342:853–6. doi:10.1126/science.1243110.
- Heasley, L.R., S.M. Markus, and J.G. DeLuca. 2017. “Wait anaphase” signals are not confined to the mitotic spindle. *Mol. Biol. Cell*. 28:1186–1194. doi:10.1091/mbc.E17-01-0036.
- Heinrich, S., E.-M. Geissen, J. Kamenz, S. Trautmann, C. Widmer, P. Drewe, M. Knop, N. Radde, J. Hasenauer, and S. Hauf. 2013. Determinants of robustness in spindle assembly checkpoint signalling. *Nat. Cell Biol.* 15:1328–39. doi:10.1038/ncb2864.
- Herbert, M., M. Levasseur, H. Homer, K. Yallop, A. Murdoch, and A. McDougall. 2003. Homologue disjunction in mouse oocytes requires proteolysis of securin and cyclin B1. *Nat. Cell Biol.* 5:1023–1025. doi:10.1038/ncb1062.
- Hoffmann, S., B. Maro, J.Z. Kubiak, and Z. Polanski. 2011. A single bivalent efficiently inhibits cyclin B1 degradation and polar body extrusion in mouse oocytes indicating robust SAC during female meiosis I. *PLoS One*. 6. doi:10.1371/journal.pone.0027143.
- Holt, J.E., S.I.R. Lane, and K.T. Jones. 2013. Time-lapse epifluorescence imaging of expressed cRNA to cyclin B1 for studying meiosis I in mouse oocytes. *Methods Mol. Biol.* 957:91–106. doi:10.1007/978-1-62703-191-2-6.
- Homer, H.A., A. McDougall, M. Levasseur, K. Yallop, A.P. Murdoch, and M. Herbert. 2005. Mad2 prevents aneuploidy and premature proteolysis of cyclin B and securin during meiosis I in mouse oocytes. *Genes Dev.* 19:202–207. doi:10.1101/gad.328105.
- Jia, L., S. Kim, and H. Yu. 2013. Tracking spindle checkpoint signals from kinetochores to APC/C. *Trends Biochem. Sci.* 38:302–311. doi:10.1016/j.tibs.2013.03.004.
- Jones, K.T., and S.I.R. Lane. 2013. Molecular causes of aneuploidy in mammalian eggs. *Development*. 140:3719–30. doi:10.1242/dev.090589.
- Kitajima, T.S., M. Ohsugi, and J. Ellenberg. 2011. Complete kinetochore

- tracking reveals error-prone homologous chromosome biorientation in mammalian oocytes. *Cell*. 146:568–581. doi:10.1016/j.cell.2011.07.031.
- Kolano, A., S. Brunet, A.D. Silk, D.W. Cleveland, and M.-H. Verlhac. 2012. Error-prone mammalian female meiosis from silencing the spindle assembly checkpoint without normal interkinetochore tension. *Proc. Natl. Acad. Sci. U. S. A.* 109:E1858-67. doi:10.1073/pnas.1204686109.
- Kyogoku, H., and T.S. Kitajima. 2017. Large Cytoplasm Is Linked to the Error-Prone Nature of Oocytes. *Dev. Cell*. 41:287–298.e4. doi:10.1016/j.devcel.2017.04.009.
- Lane, S.I., and K.T. Jones. 2014. Non-canonical function of spindle assembly checkpoint proteins after APC activation reduces aneuploidy in mouse oocytes. *Nat Commun*. 5:3444. doi:10.1038/ncomms4444.
- Lane, S.I.R., S. Crouch, and K.T. Jones. 2016. Imaging chromosome separation in mouse oocytes by responsive 3D confocal timelapse microscopy. *Methods Mol. Biol.*
- Lane, S.I.R., Y. Yun, and K.T. Jones. 2012. Timing of anaphase-promoting complex activation in mouse oocytes is predicted by microtubule-kinetochore attachment but not by bivalent alignment or tension. *Development*. 139:1947–55. doi:10.1242/dev.077040.
- Levasseur, M. 2013. Making cRNA for microinjection and expression of fluorescently tagged proteins for live-cell imaging in oocytes. *Methods Mol. Biol.* 957:121–34. doi:10.1007/978-1-62703-191-2_8.
- Liu, D., H. Shao, H. Wang, and X.J.J. Liu. 2014. Meiosis I in *Xenopus* oocytes is not error-prone despite lacking spindle assembly checkpoint. *Cell Cycle*. 13:1602–1606. doi:10.4161/cc.28562.
- McGuinness, B.E., M. Anger, A. Kouznetsova, A.M. Gil-Bernabé, W. Helmhart, N.R. Kudo, A. Wuensche, S. Taylor, C. Hoog, B. Novak, and K. Nasmyth. 2009. Regulation of APC/C Activity in Oocytes by a Bub1-Dependent Spindle Assembly Checkpoint. *Curr. Biol.* 19:369–380. doi:10.1016/j.cub.2009.01.064.
- Merriman, J. a, S.I.R. Lane, J.E. Holt, P.C. Jennings, I. García-Higuera, S. Moreno, E. a McLaughlin, and K.T. Jones. 2013. Reduced chromosome cohesion measured by interkinetochore distance is associated with aneuploidy even in oocytes from young mice. *Biol. Reprod.* 88:31.

doi:10.1095/biolreprod.112.104786.

- Minshull, J., H. Sun, N.K. Tonks, and a W. Murray. 1994. A MAP kinase-dependent spindle assembly checkpoint in *Xenopus* egg extracts. *Cell*. 79:475–486. doi:0092-8674(94)90256-9 [pii].
- Musacchio, A. 2015. The Molecular Biology of Spindle Assembly Checkpoint Signaling Dynamics. *Curr. Biol*. 25:R1002–R1018. doi:10.1016/j.cub.2015.08.051.
- Nagaoka, S.I., C.A. Hodges, D.F. Albertini, and P.A. Hunt. 2011. Oocyte-specific differences in cell-cycle control create an innate susceptibility to meiotic errors. *Curr. Biol*. 21:651–657. doi:10.1016/j.cub.2011.03.003.
- Pesenti, M.E., J.R. Weir, and A. Musacchio. 2016. Progress in the structural and functional characterization of kinetochores. *Curr Opin Struct Biol*. 37:152–163. doi:10.1016/j.sbi.2016.03.003.
- Polanski, Z., and J.Z. Kubiak. 2013. Free-hand bisection of mouse oocytes and embryos. *Methods Mol Biol*. 957:255–265. doi:10.1007/978-1-62703-191-2_18.
- Rieder, C.L., a Khodjakov, L. V Paliulis, T.M. Fortier, R.W. Cole, and G. Sluder. 1997. Mitosis in vertebrate somatic cells with two spindles: implications for the metaphase/anaphase transition checkpoint and cleavage. *Proc. Natl. Acad. Sci. U. S. A*. 94:5107–12. doi:10.1073/pnas.94.10.5107.
- Rodriguez-Bravo, V., J. Maciejowski, J. Corona, H.K. Buch, P. Collin, M.T. Kanemaki, J. V. Shah, and P. V. Jallepalli. 2014. Nuclear pores protect genome integrity by assembling a premitotic and mad1-dependent anaphase inhibitor. *Cell*. 156:1017–1031. doi:10.1016/j.cell.2014.01.010.
- Schuh, M., and J. Ellenberg. 2007. Self-Organization of MTOCs Replaces Centrosome Function during Acentrosomal Spindle Assembly in Live Mouse Oocytes. *Cell*. 130:484–498. doi:10.1016/j.cell.2007.06.025.
- Sebestova, J., A. Danylevska, L. Novakova, M. Kubelka, and M. Anger. 2012. Lack of response to unaligned chromosomes in mammalian female gametes © 2012 Landes Bioscience . Do not distribute . © 2012 Landes Bioscience . Do not distribute . 1–8.
- Shao, H., R. Li, C. Ma, E. Chen, and X.J. Liu. 2013. *Xenopus* oocyte meiosis lacks spindle assembly checkpoint control. *J. Cell Biol*. 201:191–200.

doi:10.1083/jcb.201211041.

Touati, S.A., and K. Wassmann. 2016. How oocytes try to get it right: spindle checkpoint control in meiosis. 125.

Tsafiri, a, S.Y. Chun, R. Zhang, a J. Hsueh, and M. Conti. 1996. Oocyte maturation involves compartmentalization and opposing changes of cAMP levels in follicular somatic and germ cells: studies using selective phosphodiesterase inhibitors. *Dev. Biol.* 178:393–402.

doi:10.1006/dbio.1996.0226.

Wild, T., M.S.Y. Larsen, T. Narita, J. Schou, J. Nilsson, and C. Choudhary. 2016. The Spindle Assembly Checkpoint Is Not Essential for Viability of Human Cells with Genetically Lowered APC/C Activity. *Cell Rep.* 14:1829–1840. doi:10.1016/j.celrep.2016.01.060.

doi:10.1016/j.celrep.2016.01.060.

Yu, F., Y. Jiang, L. Lu, M. Cao, Y. Qiao, X. Liu, D. Liu, T. Van Dyke, F. Wang, X. Yao, J. Guo, and Z. Yang. 2017. Aurora-A promotes the establishment of spindle assembly checkpoint by priming the Haspin-Aurora-B feedback loop in late G2 phase. *Cell Discov.* 3:16049.

doi:10.1038/celldisc.2016.49.

Zhang, M., P. Kothari, and M.A. Lampson. 2015. Spindle assembly checkpoint acquisition at the mid-blastula transition. *PLoS One.* 10:e0119285. doi:10.1371/journal.pone.0119285.

doi:10.1371/journal.pone.0119285.

Figure Legends

Figure 1. Repeated oocyte bisection produces small oocytes that undergo meiosis I. (A) Schematic of the triple bisection procedure showing the generation of B₀, B₁, B₂, and B₃ oocytes. The same colours are adopted for all figures throughout. (B) Oocyte volumes expressed in pL (left axis), or as a percentage of full size oocytes (right axis). Dashed horizontal lines show the expected sizes of half, quarter and eighth oocytes. (C) Oocyte radii after bisection. (D) Representative images of oocytes expressing Tubulin-GFP and Histone 2B-mCherry, with cartoon depiction underneath. Scale bar represents 50µm. (E) Percentage of oocytes completing meiosis I. (B,C,E) Number of oocytes used are indicated in parenthesis. (B,C) Groups without common letters indicate significant differences (ANOVA with Tukey's correction for multiple comparisons; P<0.0001).

Figure 2. Smaller oocytes spend longer in prometaphase but then have a faster rate of securin loss. (A) Relative securin degradation traces from B₃ cytoplasts lacking chromosomes following bisection. (B) Representative timelapse of B₀ (top) and B₃ (bottom) oocytes expressing Securin-YFP and Histone 2B-mCherry relative to time after NEB. Scale bar, 10µm. (C) The timing of anaphase relative to NEB, determined from images as in (B). There is no significant difference in the time of anaphase between B₀ and B₃ oocytes. (D) The timing of NEB (left) and anaphase (right) relative to activation of the APC. Plots for individual oocytes are displayed above, with means below. (E) Individual (pale) and mean (bold) securin traces from B₀ and B₃ oocytes, arranged relative to the time of APC activation. Horizontal bars show the corresponding timing of anaphase. (F) The maximal rate of securin destruction recorded from traces as in (E). (C,D,F) Number of oocytes used indicated in parenthesis. (C,D,F) Statistical test was an unpaired t-test.

Figure 3. Non-biorientated bivalents do not prevent APC activation in smaller oocytes. (A) Representative time-lapse images of B₀ and B₃ oocytes expressing Histone 2B-mCherry (green) and CenpC-GFP (red) with time relative to anaphase. Arrowheads indicate non-biorientated bivalents in both types of oocyte. Scale bar represents 10µm. (B) Cartoon depicting

measurements of stretch, displacement and θ on a bivalent with sister kinetochore pairs (red). **(C)** The number of bivalents per oocyte classed as non-biorientated (>3 standard deviations from the control mean in any of the parameters of stretch, displacement or θ) at times relative to anaphase. **(D)** 3D plot of bivalents in B_3 oocytes 5 minutes prior to anaphase, indicating the spread of stretch, displacement and θ . Colours indicate the number of standard deviations a bivalent is, according to its worst performing measure, from mean values defined by metaphase oocytes treated without nocodazole (green <1 , yellow ≤ 2 , orange ≤ 3 , red >3). **(E,F)** Proportion of bivalents falling within the stated number of standard deviations at anaphase -5 minutes for B_0 (E) and B_3 (F) oocytes.

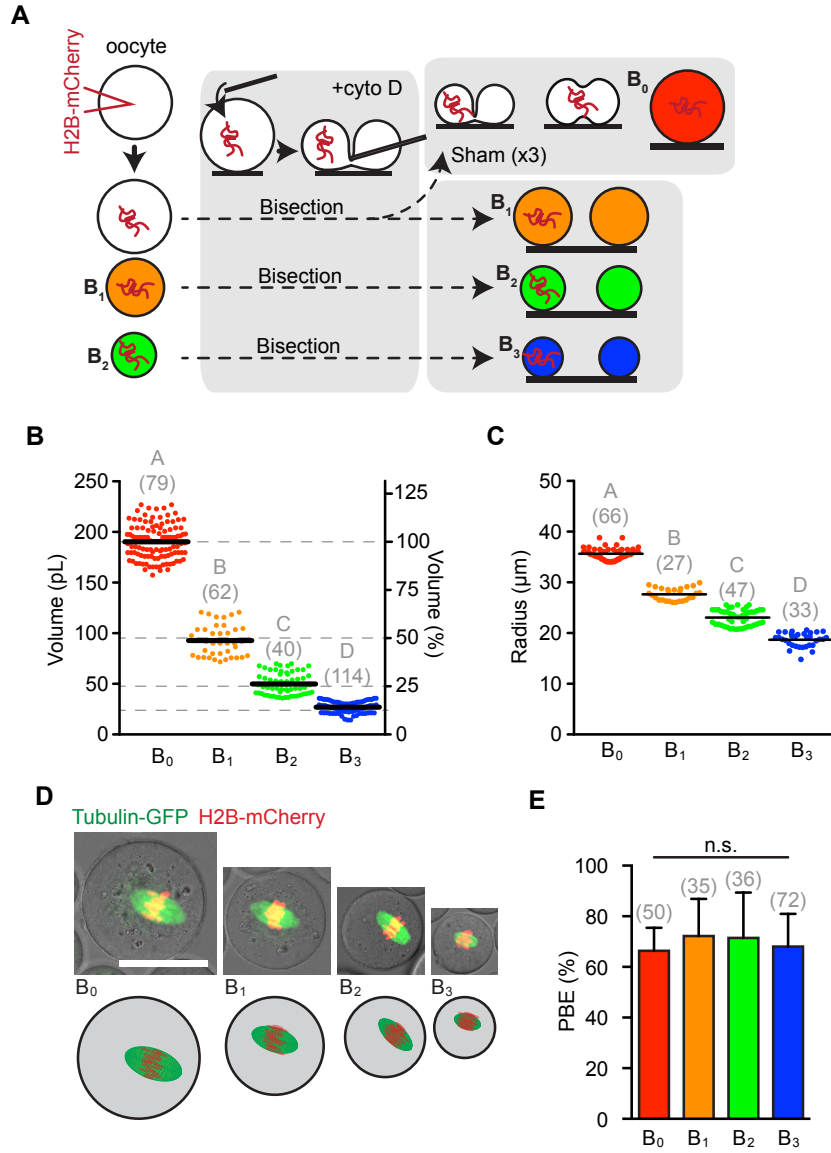
Figure 4. Several non-biorientated bivalents fail to prevent APC activation in small oocytes. **(A)** Percentage of B_0 and B_3 oocytes extruding polar bodies with or without addition of 25nM nocodazole to the culture media. Statistical test was Fisher's exact. **(B)** Representative time-lapse images of oocytes expressing Histone 2B-mCherry and CenpC-GFP with time relative to anaphase. Scale bar, 10 μ m. **(C)** The number of bivalents per oocyte classed as non-biorientated (>3 standard deviations from the control mean in any of the parameters of stretch, displacement or θ) at times relative to anaphase. Statistical test is Dunn's multiple comparison test; n.s. not significant, * $p<0.05$, ** $p<0.01$. **(D)** 3D scatterplot of bivalents 5 minutes prior to anaphase in B_3 oocytes cultured in 25nM nocodazole. Colours indicate the number of standard deviations a bivalent is, according to its worst performing measure, from mean values defined by metaphase oocytes treated without nocodazole (green <1 , yellow ≤ 2 , orange ≤ 3 , red >3). **(E)** Proportion of bivalents for B_0 oocytes falling within the stated number of standard deviations at anaphase -5 minutes.

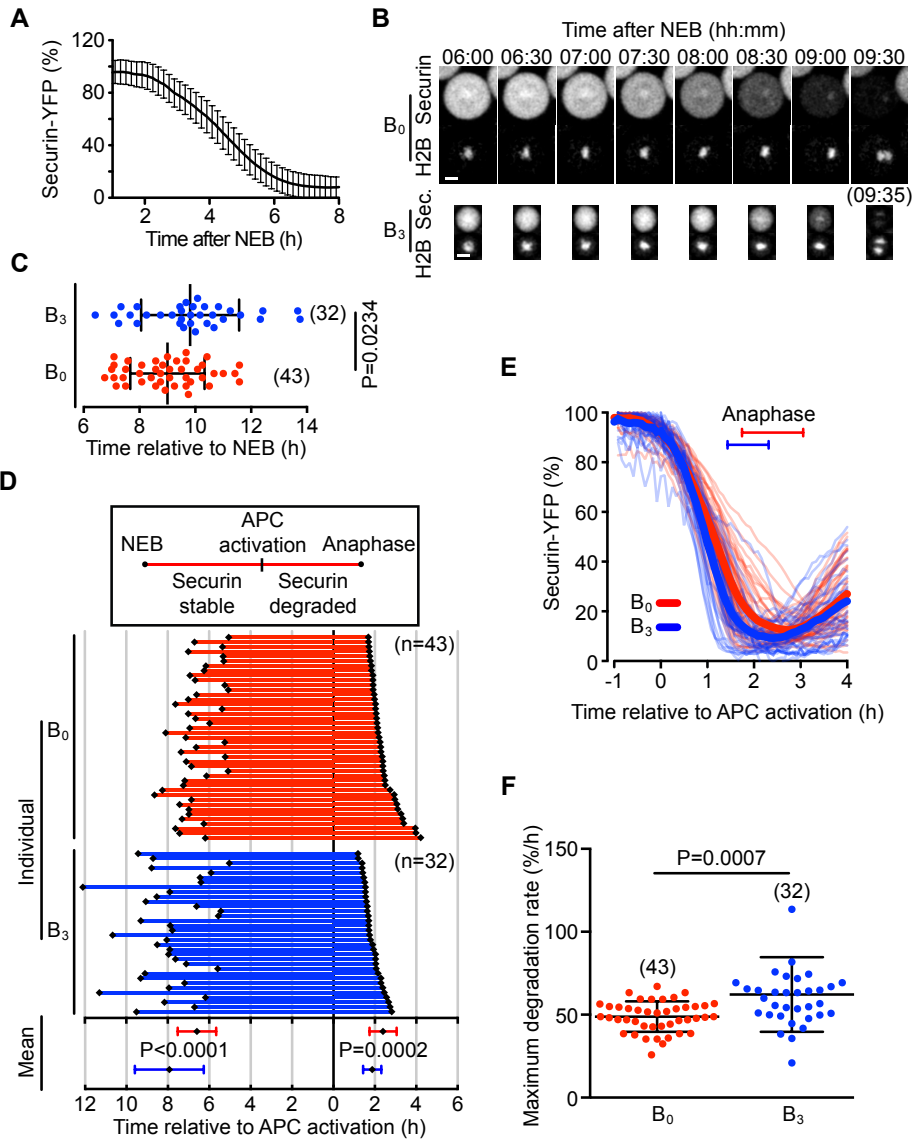
Figure 5. Matched doses of nocodazole reveal differences in APC activity with reduced oocyte volume. **(A)** B_0 oocytes were matured in the indicated concentrations of nocodazole and assessed for bivalent biorientation at 6h after NEB. Colours indicate the number of standard deviations a bivalent is, according to its worst performing measure, from mean

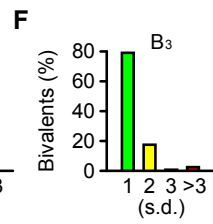
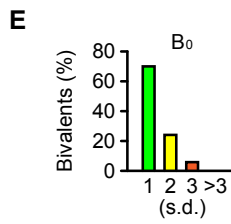
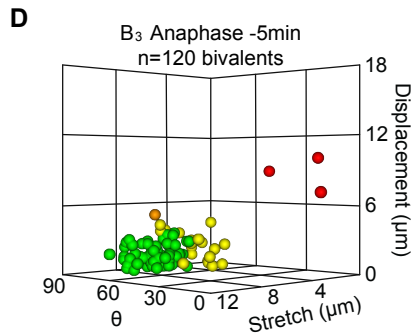
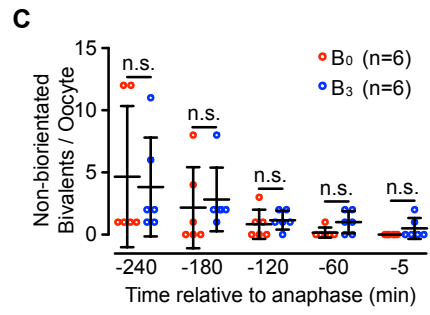
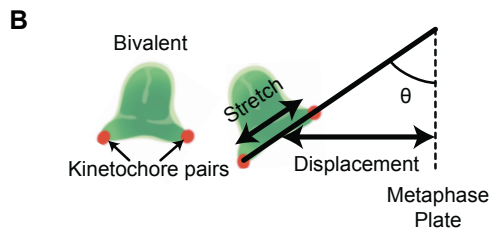
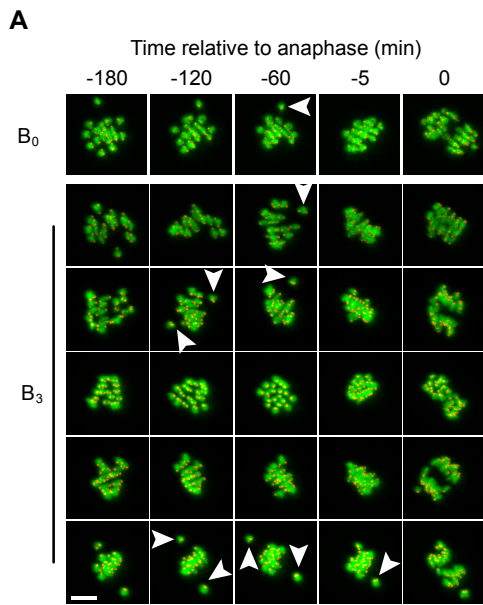
values defined by metaphase oocytes treated without nocodazole (green <1, yellow <=2, orange <=3, red >3). **(B,C)** 3D scatter plots showing the extent of chromosome biorientation in B₃ oocytes (25nM nocodazole, B) and B₀ oocytes (35nM nocodazole, C) as in A. **(D)** Percentage of oocytes of the indicated size extruding polar bodies following 15 h culture in the indicated concentration of nocodazole. **(E)** The duration of meiosis I, defined as the time from NEB to anaphase. **(F)** Individual (pale) and mean (bold) securin traces from B₀ and B₃ oocytes, arranged relative to the time of APC activation. Horizontal bars show the corresponding timing of anaphase. **(G)** Representative traces of two modes of securin degradation found in B₃ oocytes matured in 25nM nocodazole. Arrowheads indicate the timing of anaphase. Red colour indicated periods of stalling. **(H)** Proportion of MI arrested oocytes that exhibited stalling. **(I)** Proportion of oocytes that completed meiosis I that exhibited stalling. **(J)** Results from experiments with and without nocodazole addition are presented together for comparison of the effects of oocyte volume reduction and addition of matched doses of nocodazole. Blue points indicate B₃ oocytes, whilst red are B₀. Round points indicate no stalling event was detected, square points indicate stalling. Back border indicates the presence of nocodazole (25nM for B₃, 35nM for B₀). Parenthesis indicates number of oocytes. Error bars are standard deviations. Grey dashed lines indicate points where the duration of meiosis I (prometaphase + metaphase) is the same. Statistical comparisons between all points are indicated in Figure S3. (A,D,E,G-I) number of oocytes indicated in parenthesis. Statistical test used were Fishers exact test (D, H, I), Unpaired t-test (E).

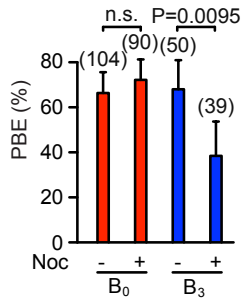
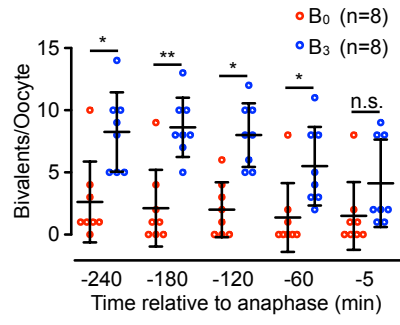
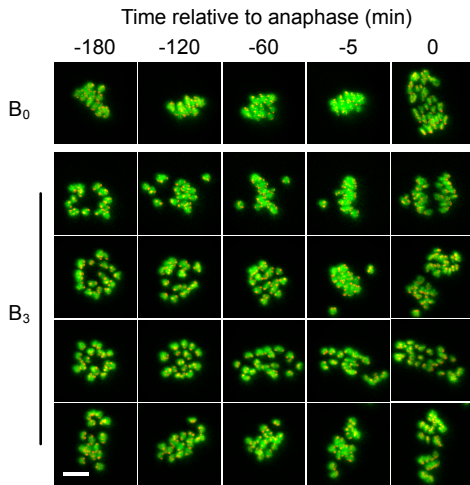
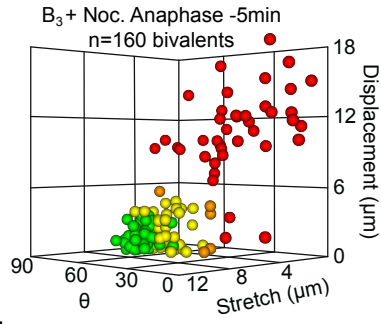
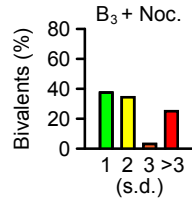
Abbreviations List

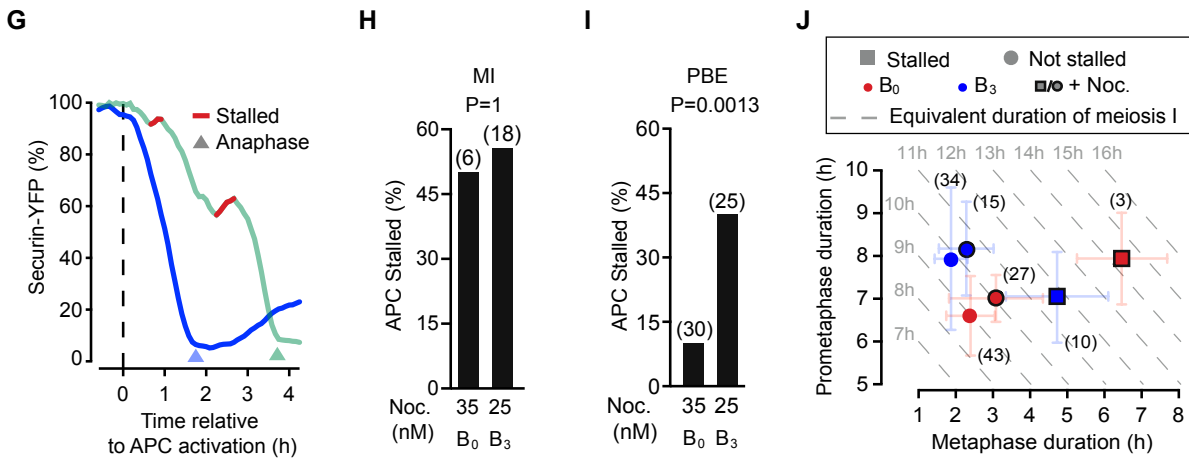
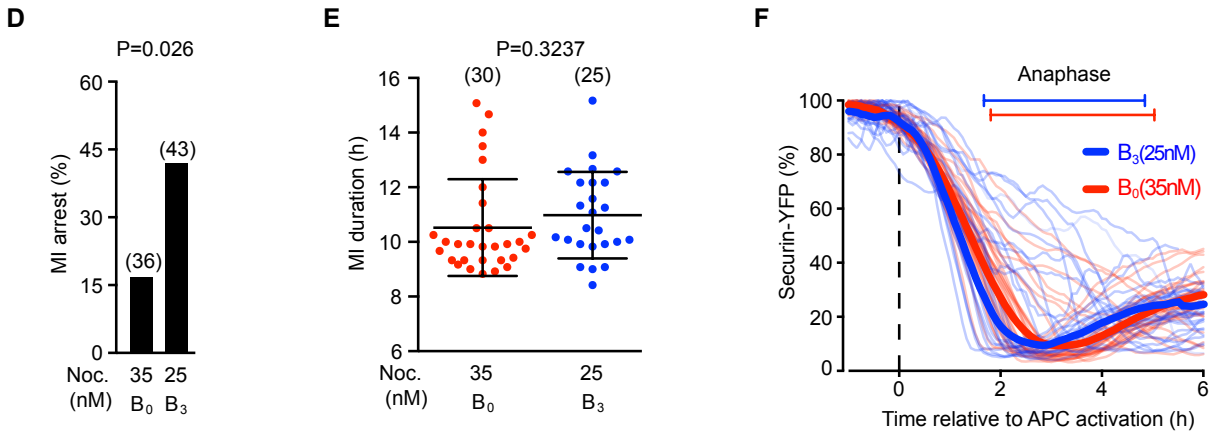
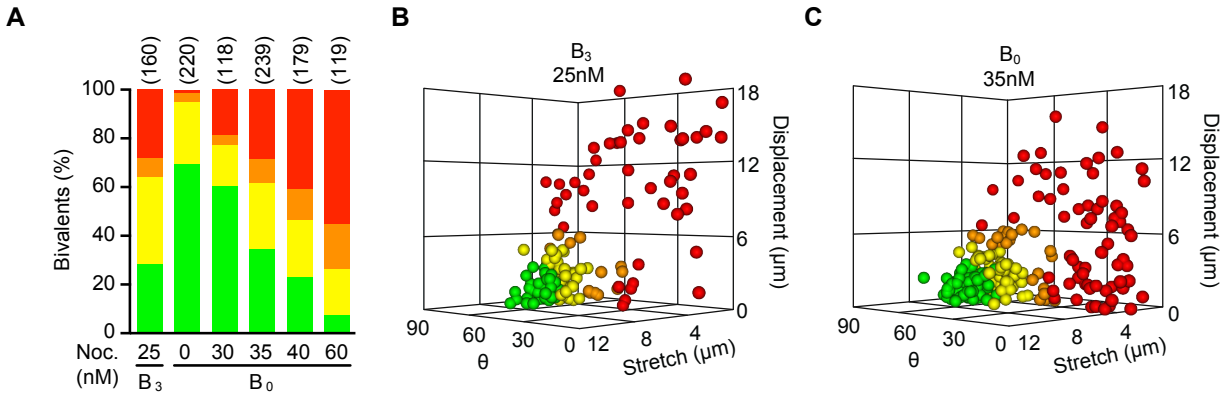
4D-CSLM	4-dimensional Confocal Scanning Laser Microscopy
ANOVA	ANalysis Of VAriance
APC	Anaphase Promoting Complex
B ₀	Sham bisected
B ₁	Bisected once
B ₂	Bisected twice
B ₃	Bisected three times
CenpC	Centromere protein C
cRNA	complementary RiboNucleic Acid
DIC	Difference Interference Contrast
GFP	Green Fluorescent Protein
H2B	Histone 2B
NEB	Nuclear Envelope Breakdown
PBE	Polar Body Extrusion
SAC	Spindle Assembly Checkpoint
YFP	Yellow Fluorescent Protein

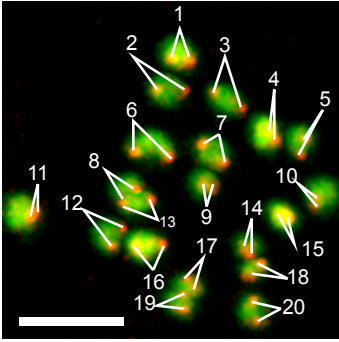
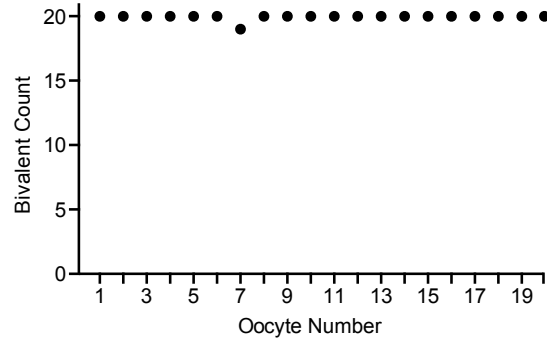
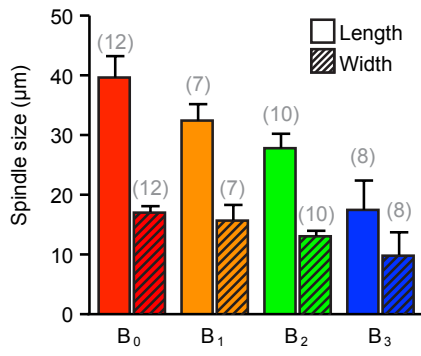






A**C****B****D****E**



A**B****C****D**